

Uniformly Distributed Fe₂O₃ Nanoparticles' Thin Films Synthesized by Spray Pyrolysis

Dayanand^{1,\$}, Meenu Chahar^{1,\$}, Devesh Kumar Pathak^{2,\$}, O. P.Thakur^{*1} , V. D. Vankar¹ and
Rajesh Kumar^{2,*}

¹Material Analysis and Research Laboratory, Department of Physics, Netaji Subhas University of
Technology, New Delhi- 110078, India

²Materials and Device Laboratory, Discipline of Physics, Indian Institute of Technology Indore, Simrol,
Indore-453552, India

^{\$} Authors contributed equally

*Email: rajeshkumar@iiti.ac.in (Rajesh Kumar); opthakur@nsut.ac.in (O.P. Thakur).

Abstract

Thin films of uniformly distributed Fe_2O_3 nanoparticles have been prepared on single crystal silicon and glass substrates by a spray pyrolysis technique in a single step using a mixture of water and ferrocene dissolved in xylene. The size distribution of nanoparticles is found to be in the range of 20 nm to 30 nm. The films have been characterized by X-ray diffraction, scanning electron microscopy and Raman spectroscopy techniques. The uniformity of the grown film was evident from the electron microscopic images on both the substrates. The crystallinity and band gap were investigated using X-ray diffraction and absorption spectroscopy respectively. Raman measurements of the prepared films have been carried out using two excitation wavelengths of 633 nm and 785 nm to investigate the depth of homogeneity of the films. The wavelength dependent Raman measurements reveal that the film is uniform across the thickness of the film on both the substrates.

Keywords: *Spray pyrolysis; Ferrocene; Hematite; Nanoparticles; Thin films.*

Introduction

In recent years, iron oxide (Fe_2O_3) has attracted much attention as its different structural and morphological forms have found several technological applications such as magnetic storage devices, magnetic fluid devices, pigments, catalysis, electromagnetic shielding etc[1–5]. Iron oxide exists in different structural forms viz- rhombohedral α - Fe_2O_3 (hematite JCPDS-card No. 89-0597), cubic α - Fe_2O_3 (maghemite JCPDS- card No.39-1346) and Fe_3O_4 (magnetite JCPDS card No.19-0629). These structural forms exist in different temperature ranges and exhibit different physical and chemical properties. These materials can be synthesized by variety of techniques using different precursors and have variety of applications [6–17]. Some of the technological applications and synthesis processes used by different workers are given in the table no.3 below. It is observed that very fine powders, or hollow spheres[5,10] can be grown by hydro-thermal process[7,18–23] or by spray pyrolysis[14] in large amounts whereas good quality oxide films having great adhesion to the substrate can be prepared using electro-deposition methods[24]. The co- precipitation process is used to obtain core-shell nano-particles[3]. Heat treatment of iron substrates leads to growth of large arrays of vertically aligned nano-rods of Fe_2O_3 [11]. These particles do have different orders of crystallinity[12,13,15]. The kinetics of growth of some of these different structures has been studied by Jorgensen et.al[8]. Since, the morphology, microstructures and the crystallinity are critical factors to bring novel and unique size and shape dependent functional properties, significant attention has been paid for controlled synthesis of nano- materials employing different techniques and variety of pre-cursors. Most of these techniques involve cumbersome routes and complex chemical reactions of the pre- cursers involved. Recently Gonzalez- Carreno et al.[15] have used spray pyrolysis technique to prepare uniform sized γ - Fe_2O_3 particles of different degree of crystallinity using different precursors such as Fe-acetylacetonone, Fe-ammonium citrate, Fe- nitrate and Fe-chloride dissolved in methanol. They have also shown that α - Fe_2O_3 can be prepared in a single step by combustion of iron nitrate and malonic acid dihydrazide by spray pyrolysis technique. Pressure pyrolysis technique has been used by Hirano et al.[16] for synthesis of ferrite- carbon composites using nickelocene and

vinylferrocene as pre-cursors. This technique, however, employs very high pressures (30-200 MPa) and high temperatures (500- 700°C) in a hydrothermal growth apparatus. Spray pyrolysis is a widely used technique for producing micro-and nano-scale particles of varying size distributions from materials of various kind such as metals, oxides semiconductors etc. Because of its convenient process characteristics compared to other methods like physical and chemical vapour deposition, plasma assisted vapor deposition, laser ablation etc., spray pyrolysis has found tremendous attention in recent times. Spray pyrolysis is a simple and low cost technique capable of providing large area high quality adherent films of uniform thickness. In this process, simple pre-cursors could be used to obtain fine particles or uniform coatings over large area in a single step avoiding complicated processes and complex chemical reagents.

Basic technique involved in the spray pyrolysis process is the pyrolytic decomposition of salts of a desired compound to be deposited. The spray process involves atomization of the aqueous (or solvent) pre-cursor solution into a spray of fine droplets through a fine nozzle. These droplets undergo volume expansion during their flight from the nozzle towards the hot substrate due to a temperature gradient between the two. As the droplets arrive on the hot substrate they further expand and burst into finer droplets which undergo pyrolytic decomposition and pulverization into nano-sized crystallites[17]. The substrates provide thermal energy for the thermal decomposition and subsequent recombination of the constituent species followed by sintering, nucleation, growth and crystallization, resulting in a uniform coherent and continuous thin film (Figure1a and1b).

In this paper, a single step spray pyrolysis method for preparation of thin films of α -Fe₂O₃, consisting of uniformly distributed nano- particles is reported. The films have been deposited on silicon and glass substrates by using a solution of ferrocene dissolved in xylene mixed with water. The phase identification and microstructure analysis has been carried out by X-ray diffraction (XRD), Raman spectroscopy and scanning electron microscopic (SEM)

techniques. Raman spectroscopy has been carried out using two excitation wavelengths to examine the homogeneity along the film depth. The α -Fe₂O₃ film deposited on glass substrate was used to estimate the band gap of the film using absorption spectroscopy.

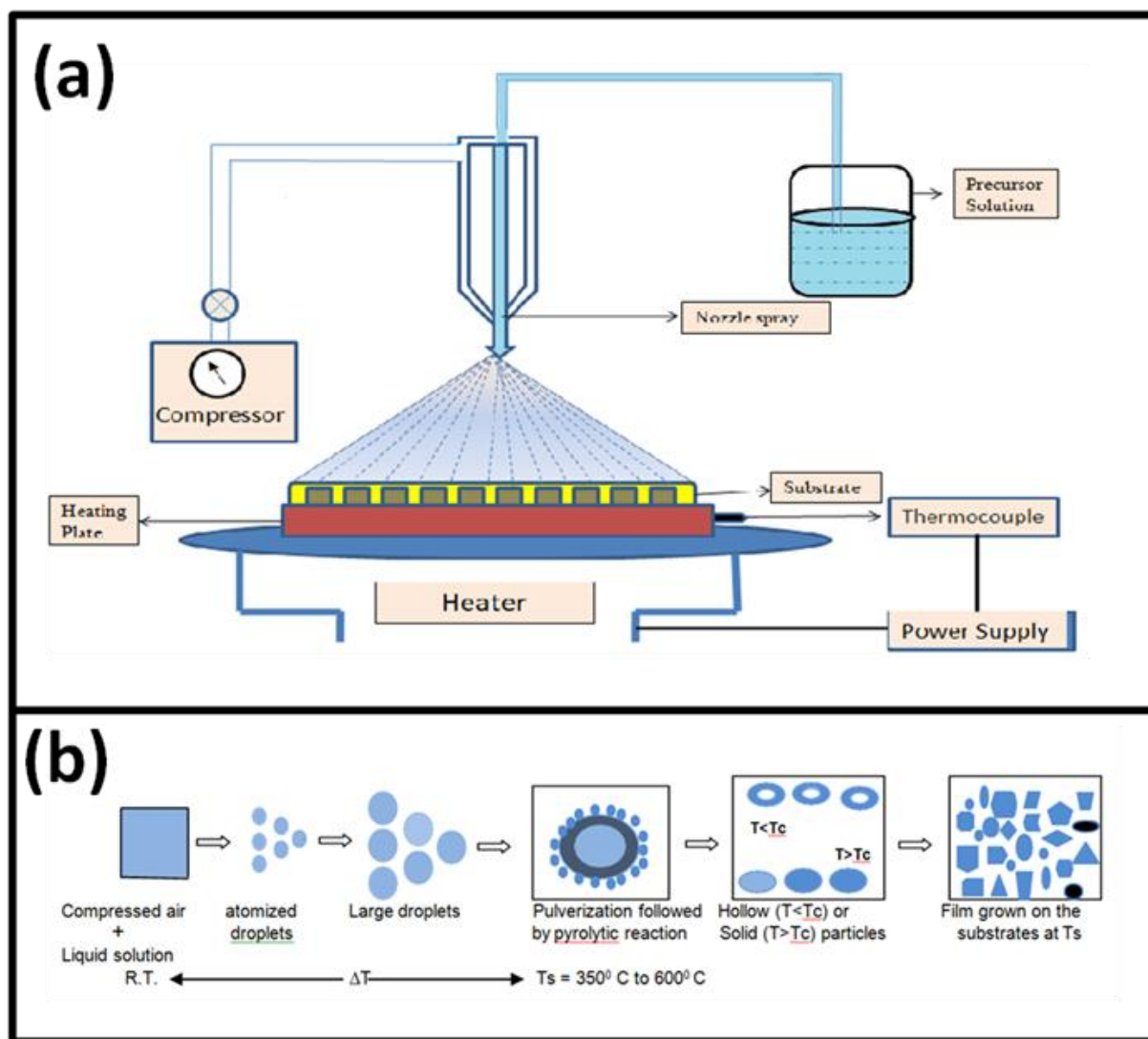


Figure 1: (a) Schematic diagram of the spray pyrolysis set up used for deposition of uniform thin films over large area. It consists of a shielded heater plate, heat shield plate, temperature controller, liquid dispenser attached to a spray nozzle- atomizer and an air compressor. (b) A schematic representation of the mechanism of nano-particle formation by the spray pyrolysis process.

Experimental Details

The films of α - Fe_2O_3 were prepared by spray pyrolysis by an apparatus shown in Figure(1a). Ferrocene was dissolved in xylene (solubility $\sim 13\%$) and equal amount of pure water was added into this solution to form a suspension. The suspension (composition : 2.5 gms. of ferrocene dissolved in 125 mL of xylene and 125 mL of pure water) was continuously stirred and fed into the spray nozzle (orifice diameter ~ 0.2 mm) and atomizer system to generate very fine droplets which were directed on a number of heated substrates kept on a hot plate maintained at constant temperature. The nozzle to substrate distance was ~ 25 cm forming a cone of diameter 20 cm on the substrate plate. The solution was sprayed for ~ 20 minutes. Thin films were deposited on both glass (1 mm thick) and silicon single crystal wafers (300 μm thick) kept on the same heater plate. The temperature of the substrates was monitored by using a chromel –alumel thermocouple. The measured temperature on the silicon substrate was 500°C and that on the glass substrate surface was 480°C . After the deposition process, the heater was switched off and allowed to cool till room temperature was achieved. The time needed was ~ 2 hours. The films were annealed at gradually decreasing temperatures under ambient conditions. The films (~ 100 nm thick) were then taken out for SEM, XRD, UV-Visible and Raman spectroscopy analysis.

The thin films of Fe_2O_3 on silicon as well as glass substrates were examined under a Zeiss FE SEM model Supra Z5 in the secondary electron mode with excitation voltage 5 kV and working distance of 3.3 mm. The X-ray diffraction data was recorded using Rigaku Smart Lab monochromatic $\text{Cu-K}\alpha$ radiation ($\lambda=1.54 \text{ \AA}$) in glancing angle diffraction mode keeping the incidence angle $\alpha = 2^\circ$ (Figure 2). The Raman spectra were recorded using Horiba Labram HR evolution laser He-Ne laser ($\lambda_{\text{ex}}= 633 \text{ nm}$ and 785 nm).

Results and Discussion

Figure 2a and 2b show typical scanning electron micrographs of these samples on silicon and glass substrates respectively. The micrograph (Figure 2a) shows uniform and dense distribution of small clusters consisting of particles of random shape and size between 20 nm to 30 nm. The micrograph in Figure 2(b) shows uniformly distributed larger clusters consisting of particles of random shape and size between 20 nm to 50 nm. These particles are not so densely distributed as compared to those deposited on silicon substrates (Figure 2a). The difference in size and distribution is attributed to difference in the substrate temperature at which the pyrolysis was carried out viz at 500 °C on silicon and 480 °C on glass substrates.

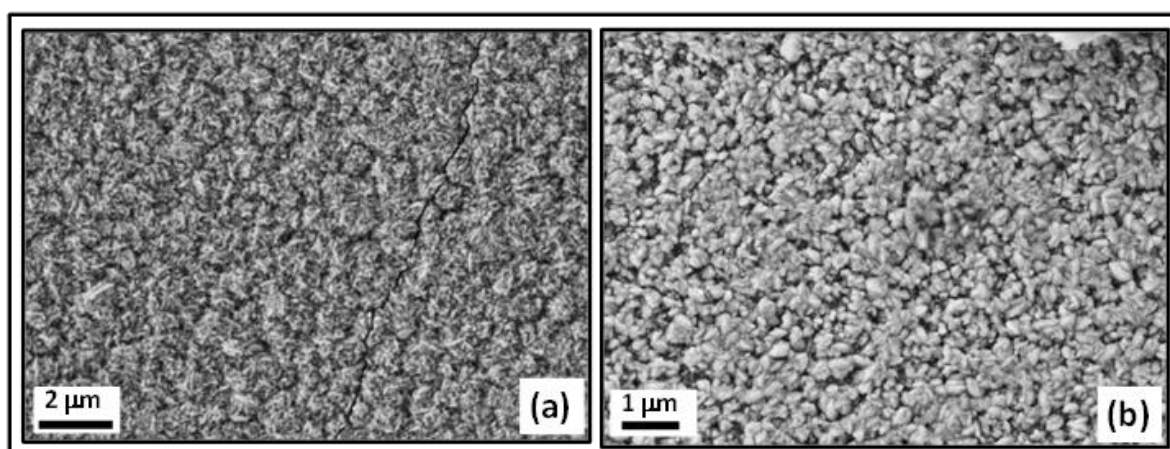


Figure 2: SEM micrographs of α -Fe₂O₃ thin films deposited on (a) silicon single crystal substrate at 500 °C and (b) glass substrate at 480 °C.

Figure 3 shows XRD patterns of the films deposited on silicon and glass substrates respectively. All the peaks could be identified with the hexagonal phase of α -Fe₂O₃ with structural parameters of $a = b = 5.034 \text{ \AA}$ and $c = 13.721 \text{ \AA}$, which are in good agreement with the literature (JCPDS card no. 33-0664). It is reported that pure α -Fe₂O₃ phase exists in rhombohedral form (JCPDS No. 89-0597) with a small amount of carbon in graphitic form. The

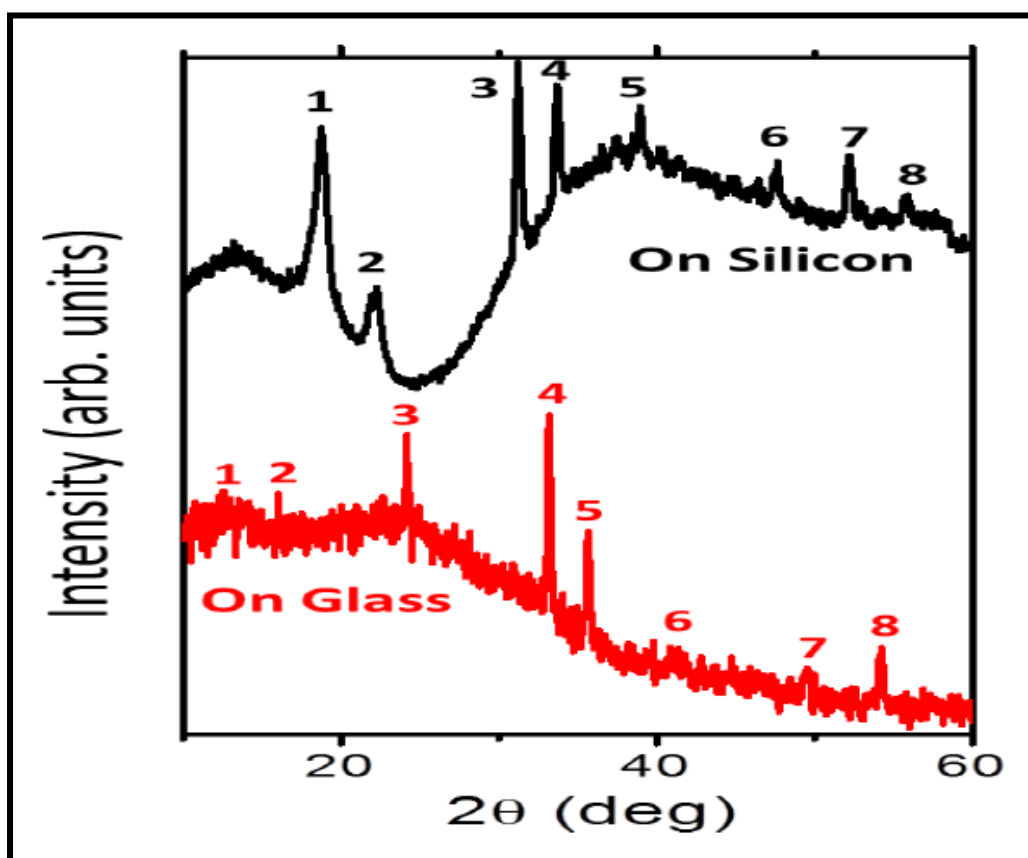


Figure 3: X-ray diffraction patterns of films deposited on (a) silicon substrate and (b) glass substrate. The data was recorded using Cu-K α radiation in glancing angle diffraction mode keeping incidence angle $\alpha = 2^\circ$.

detail of analysis is presented in Table-1. Since in our synthesis process both carbon and oxygen could be present in trace amounts they could be responsible for stabilizing the hexagonal phase with slightly increased lattice parameter values as compared to those reported in the literature. XRD patterns do not show any evidence of carbon present in the films. Some of the peaks are identified as due to silicon which is coming from the single crystal silicon substrate.

Figure 4 shows the Raman spectra from the deposited films on both the substrates recorded using two excitation wavelengths of 633 nm (left panel) and 785 nm (right panel). The peaks observed in Raman spectra in Figure 4(a) and 4(b) have been compared with the data in the literature and-

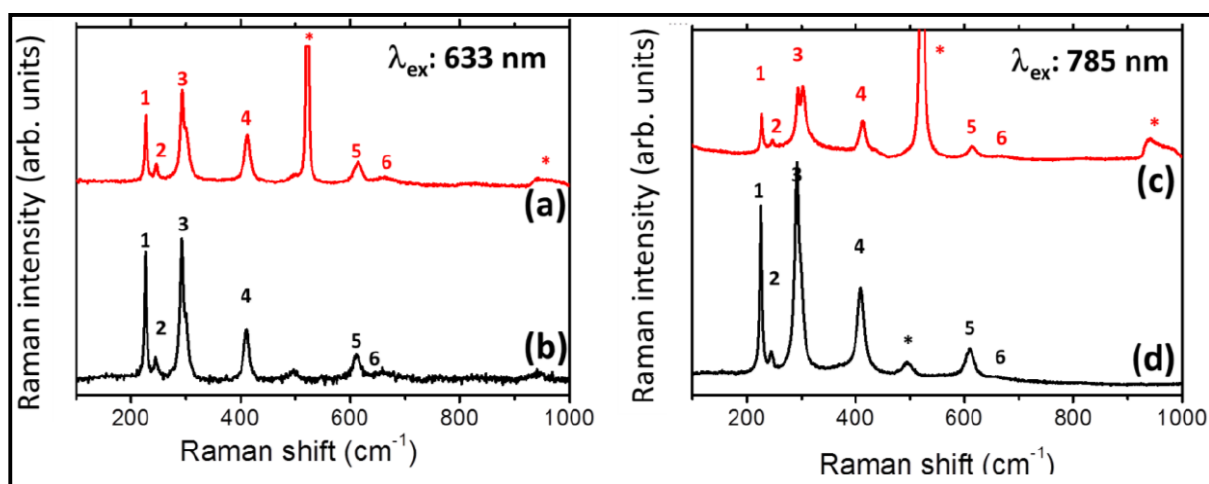


Figure 4: Raman spectra, recorded using excitation wavelength of 633 nm (left panel) and 785 nm (right panel), of films deposited on silicon substrates (a,c) and on glass substrates (b,d).

-summarized in Table 2. The films on both the substrates show Raman peaks corresponding to two A_{1g} and five E_g modes belonging to $\alpha\text{-Fe}_2\text{O}_3$. No evidence of carbon could be identified in these films. The Raman peaks corresponding to the substrates have been marked with (*). A careful analysis at the Raman data can be carried out to obtain more information related to the homogeneity of the sample. A comparison between the Raman spectra in Figure 4a with 4c and Figure 4b with 4d reveals that Raman modes are identical and has no effect of excitation wavelength. It is important here to mention that the two excitation wavelengths will have different penetration depths in the sample and thus the spectra contain information up to this depth. Considering that, excitation wavelength immune Raman signal means the presence of same material up to the sample depth penetrated by the excitation wavelength. It means that the $\alpha\text{-Fe}_2\text{O}_3$ film deposited on either of the substrates is uniform along the depth. The band gap of $\alpha\text{-Fe}_2\text{O}_3$ film deposited on the glass substrate was calculated based on its UV-Vis absorption spectrum (Figure 5) and estimated to be 3.24 eV. A high band gap value of the deposited film indicates the insulating nature of the film deposited on glass substrate.

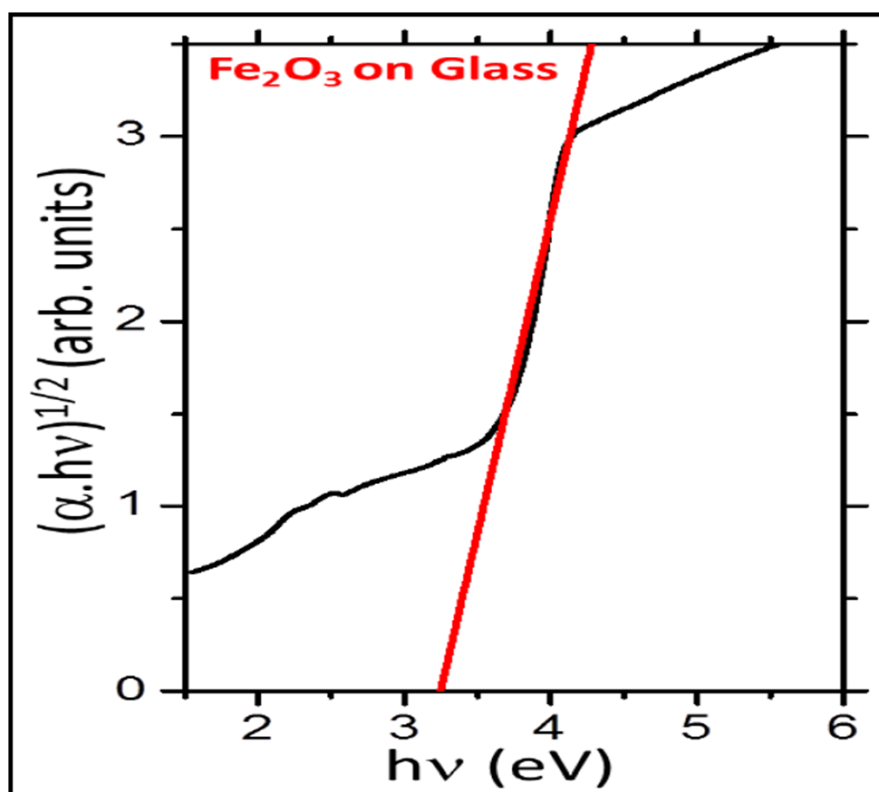


Figure 5: UV-Vis spectrum (black curve) of film deposited on glass where the red line shows the straight line fit used to estimate the band gap.

A comparison of the structural, crystallographic and optical spectroscopic (UV-Vis and Raman) data reveals that a uniform film, consisting of α - Fe_2O_3 nanostructures, can be prepared using spray pyrolysis. The film, so prepared, has a band gap of 3.24 eV and is homogeneous along the depth of the film

Conclusions

Spray pyrolysis has successfully been used for deposition of dense thin films of uniformly distributed α - Fe_2O_3 nano-particles on crystalline as well as amorphous substrates as revealed from the morphological studies. The single step spray pyrolysis process reported here uses a mixture of water and ferrocene dissolved in xylene. The structural analysis carried out using XRD, shows that Fe_2O_3 nano-particles have a single phase hematite structure stabilized with trace amount of carbon. Optical absorption spectroscopy was used to estimate the band gap of

the deposited film on glass substrate which yields band gap of 3.24 eV indicating an insulating behavior. An excitation wavelength dependent Raman spectroscopy was used to check planar and depth homogeneity and to validate phases which were found consistent with the XRD analysis. In brief, the comparison of structural, morphological and spectroscopic results concludes that a uniform film, consisting of α -Fe₂O₃ nanostructures, can be prepared using spray pyrolysis. The films, so prepared, have a relatively high band gap and are homogeneous along the depth of the films.

Acknowledgements

The authors are thankful to the Vice Chancellor, Netaji Subhas University of Technology, New Delhi for financial support. Authors acknowledge SIC facility (IIT Indore) for various measurements. One of the authors (D.K.P.) acknowledges Council of Scientific and Industrial Research (CSIR) for financial assistance (File No. 09/269 1022(0039)/2017-EMR-I). Facilities received from Department of Science and Technology (DST), Government of India, under FIST scheme (Grant SR/FST/PSI-225/2016) is highly acknowledged. Authors acknowledges financial support from Science and Engineering Research Board, Govt. of India (Grant no. CRG/2019/000371).

References

- [1] A. Namai, M. Yoshikiyo, K. Yamada, S. Sakurai, T. Goto, T. Yoshida, T. Miyazaki, M. Nakajima, T. Suemoto, H. Tokoro, S. Ohkoshi, Hard magnetic ferrite with a gigantic coercivity and high frequency millimetre wave rotation, *Nature Communications*. 3 (2012) 1–6. <https://doi.org/10.1038/ncomms2038>.
- [2] P. Tartaj, T. González- Carreño, C.J. Serna, Single-Step Nanoengineering of Silica Coated Maghemite Hollow Spheres with Tunable Magnetic Properties, *Advanced Materials*. 13 (2001) 1620–1624. [https://doi.org/10.1002/1521-4095\(200111\)13:21<1620::AID-ADMA1620>3.0.CO;2-Z](https://doi.org/10.1002/1521-4095(200111)13:21<1620::AID-ADMA1620>3.0.CO;2-Z).

- [3] N. Mufti, T. Atma, A. Fuad, E. Sutadji, Synthesis and characterization of black, red and yellow nanoparticles pigments from the iron sand, AIP Conference Proceedings. 1617 (2014) 165–169. <https://doi.org/10.1063/1.4897129>.
- [4] Y. Wu, G. Jiang, H. Zhang, Z. Sun, Y. Gao, X. Chen, H. Liu, H. Tian, Q. Lai, M. Fan, D. Liu, Fe₂O₃, a cost effective and environmentally friendly catalyst for the generation of NH₃ – a future fuel – using a new Al₂O₃-looping based technology, Chem. Commun. 53 (2017) 10664–10667. <https://doi.org/10.1039/C7CC04742H>.
- [5] H. Wu, G. Wu, L. Wang, Peculiar porous α -Fe₂O₃, γ -Fe₂O₃ and Fe₃O₄ nanospheres: Facile synthesis and electromagnetic properties, Powder Technology. 269 (2015) 443–451. <https://doi.org/10.1016/j.powtec.2014.09.045>.
- [6] J. Lian, X. Duan, J. Ma, P. Peng, T. Kim, W. Zheng, Hematite (α -Fe₂O₃) with Various Morphologies: Ionic Liquid-Assisted Synthesis, Formation Mechanism, and Properties, ACS Nano. 3 (2009) 3749–3761. <https://doi.org/10.1021/nn900941e>.
- [7] J. Li, R. Hong, G. Luo, Y. Zheng, H. Li, D. Wei, An easy approach to encapsulating Fe₃O₄ nanoparticles in multiwalled carbon nanotubes, New Carbon Materials. 25 (2010) 192–198. [https://doi.org/10.1016/S1872-5805\(09\)60026-3](https://doi.org/10.1016/S1872-5805(09)60026-3).
- [8] J.-E. Jørgensen, L. Mosegaard, L.E. Thomsen, T.R. Jensen, J.C. Hanson, Formation of γ -Fe₂O₃ nanoparticles and vacancy ordering: An in situ X-ray powder diffraction study, Journal of Solid State Chemistry. 180 (2007) 180–185. <https://doi.org/10.1016/j.jssc.2006.09.033>.
- [9] Q. Gao, F. Chen, J. Zhang, G. Hong, J. Ni, X. Wei, D. Wang, The study of novel Fe₃O₄@ γ -Fe₂O₃ core/shell nanomaterials with improved properties, Journal of Magnetism and Magnetic Materials. 321 (2009) 1052–1057. <https://doi.org/10.1016/j.jmmm.2008.10.022>.
- [10] Y. Wang, J.-L. Cao, M.-G. Yu, G. Sun, X.-D. Wang, H. Bala, Z.-Y. Zhang, Porous α -Fe₂O₃ hollow microspheres: Hydrothermal synthesis and their application in ethanol sensors, Materials Letters. 100 (2013) 102–105. <https://doi.org/10.1016/j.matlet.2013.03.037>.
- [11] Y.Y. Fu, R.M. Wang, J. Xu, J. Chen, Y. Yan, A.V. Narlikar, H. Zhang, Synthesis

- of large arrays of aligned α -Fe₂O₃ nanowires, *Chemical Physics Letters*. 379 (2003) 373–379. <https://doi.org/10.1016/j.cplett.2003.08.061>.
- [12] C. Baratto, P.P. Lottici, D. Bersani, G. Antonioli, G. Gnappi, A. Montenero, Sol-Gel Preparation of α -Fe₂O₃ Thin Films: Structural Characterization by XAFS and Raman, *Journal of Sol-Gel Science and Technology*. 13 (1998) 667–671. <https://doi.org/10.1023/A:1008694519106>.
- [13] D. Bersani, P.P. Lottici, A. Montenero, Micro-Raman investigation of iron oxide films and powders produced by sol–gel syntheses, *Journal of Raman Spectroscopy*. 30 (1999) 355–360. [https://doi.org/10.1002/\(SICI\)1097-4555\(199905\)30:5<355::AID-JRS398>3.0.CO;2-C](https://doi.org/10.1002/(SICI)1097-4555(199905)30:5<355::AID-JRS398>3.0.CO;2-C).
- [14] A.M. Gadalla, H.-F. Yu, Thermal decomposition of Fe(III) nitrate and its aerosol, *Journal of Materials Research*. 5 (1990) 1233–1236. <https://doi.org/10.1557/JMR.1990.1233>.
- [15] T. González-Carreño, M.P. Morales, M. Gracia, C.J. Serna, Preparation of uniform γ -Fe₂O₃ particles with nanometer size by spray pyrolysis, *Materials Letters*. 18 (1993) 151–155. [https://doi.org/10.1016/0167-577X\(93\)90116-F](https://doi.org/10.1016/0167-577X(93)90116-F).
- [16] S.-I. Hirano, T. Yogo, K.-I. Kikuta, M. Fukuda, Synthesis of nickel ferrite-dispersed carbon composites by pressure pyrolysis of organometallic polymer, *JOURNAL OF MATERIALS SCIENCE*. 28 (1993) 4073–4077. <https://doi.org/10.1007/BF00351235>.
- [17] M. Eslamian, M. Ahmed, N. Ashgriz, Modelling of nanoparticle formation during spray pyrolysis, *Nanotechnology*. 17 (2006) 1674–1685. <https://doi.org/10.1088/0957-4484/17/6/023>.
- [18] S. Mishra, P. Yogi, S.K. Saxena, J. Jayabalan, P. Behera, P.R. Sagdeo, R. Kumar, Significant field emission enhancement in ultrathin nano-thorn covered NiO nano-petals, *J. Mater. Chem. C*. (2017). <https://doi.org/10.1039/C7TC01949A>.
- [19] S. Mishra, S. Lambora, P. Yogi, P.R. Sagdeo, R. Kumar, Organic Nanostructures on Inorganic Ones: An Efficient Electrochromic Display by Design, *ACS Appl. Nano Mater.* (2018). <https://doi.org/10.1021/acsanm.8b00871>.

- [20] S. Mishra, P. Yogi, P.R. Sagdeo, R. Kumar, TiO₂–Co₃O₄ Core–Shell Nanorods: Bifunctional Role in Better Energy Storage and Electrochromism, *ACS Appl. Energy Mater.* 1 (2018) 790–798. <https://doi.org/10.1021/acsaem.7b00254>.
- [21] D.K. Pathak, A. Chaudhary, S. Mishra, P. Yogi, S.K. Saxena, P.R. Sagdeo, R. Kumar, Precursor concentration dependent hydrothermal NiO nanopetals: Tuning morphology for efficient applications, *Superlattices and Microstructures.* 125 (2019) 138–143. <https://doi.org/10.1016/j.spmi.2018.11.001>.
- [22] D.K. Pathak, A. Chaudhary, S. Mishra, P. Yogi, P.R. Sagdeo, R. Kumar, Improved field emission from appropriately packed TiO₂ nanorods: Designing the miniaturization, *Superlattices and Microstructures.* 126 (2019) 1–7. <https://doi.org/10.1016/j.spmi.2018.12.003>.
- [23] D.K. Pathak, S. Mishra, A. Chaudhary, M. Tanwar, P. Yogi, P.R. Sagdeo, R. Kumar, Improved analytical framework for quantifying field emission from nanostructures, *Materials Chemistry and Physics.* (2020) 122686. <https://doi.org/10.1016/j.matchemphys.2020.122686>.
- [24] D.K. Pathak, A. Chaudhary, M. Tanwar, U.K. Goutam, R. Kumar, Nano-cobalt oxide/viologen hybrid solid state device: Electrochromism beyond chemical cell, *Appl. Phys. Lett.* 116 (2020) 141901. <https://doi.org/10.1063/1.5145079>.

Table 1: Analysis of XRD Pattern for Fe₂O₃ deposited on silicon and glass substrates

Sl. No.	2 θ values on Silicon Substrate (observed)	Sl. No.	2 θ values on Glass Substrate (observed)	Assigned hkl values of Fe ₂ O ₃ (JCPDF)	Assigned hkl values of Silicon
1	18.909	1	12.364	--	--
2	22.303	2	16.026	--	--
3	31.333	3	24.122	24.138 (012)	--
4	33.848	4	33.265	33.153 (104)	28.444 (111)
5	39.000	5	35.660	35.612 (110)	--
6	47.666	6	41.250	40.855 (113)	--
7	52.181	7	49.815	49.480 (024)	47.306 (220)
8	55.969	8	54.386	54.091 (116)	--
	--		--	57.429 (122)	56.126 (311)
	--		--	57.590 (018)	--

Table 2: Analysis of Raman Spectra for Fe₂O₃ deposited on Silicon and Glass substrates recorded using excitation wavelength of 633 nm.

Sl. No.	Observed Raman Peak positions on Silicon Substrate (cm ⁻¹)	Sl. No.	Observed Peak positions on Glass Substrate (cm ⁻¹)	From Ref. 29 (cm ⁻¹)	From Ref. 25 (cm ⁻¹)	Mode Assignment Ref. 29 & 25
1	225	1	225	226.5	223	A _{1g}
2	249.3	2	241.5	245.5		E _g
3	294.1	3	294.1	293.5	291	E _g
4	414.9	4	411	413	409	E _g
5	612.6	5	612.6	612.5	596	E _g
6	661.3	6	661.3	659		Disorder (?)

Table 3: Synthesis of different structural /morphological forms of Fe₂O₃ and their applications:

Sl. No.	Structure/ Morphological form	Synthesis method	Pre-cursors used	Property	Application	Reference
1	Ultra fine Fe ₂ O ₃ and Fe ₃ O ₄ powders	Hydrothermal method	Solution of ammonium and iron sulphates in presence of hydrazine	Formation of oxide powders	--	7
2	γ- Fe ₂ O ₃ nanoparticles	Thermal decomposition	Iron nitride reacted with lauric acid	Kinetics of growth and vacancy ordering	--	8
3	Core-shell nano-particles of Fe ₂ O ₃	Co-precipitation	Ferric chloride/HCl/H ₂ O ferrous chloride hydrate/ NaOH mixture	Magnetic Properties	--	9
4	Porous hollow micro- and nano- spheres	Calcination of nano-rods prepared through hydrothermal route	α-FeOOH	Dielectric and Magnetic loss	Electromagnetic shielding	10
5	Hollow spheres of Fe ₂ O ₃	Hydrothermal method	Ferric nitrate, oxalic acid and urea		Gas sensors	11
6	Large arrays of vertically aligned nano-wires	Heat treatment of iron substrates in oxidizing atmosphere	Iron substrates	High surface density	Nanodevices, catalysis	12
7	Thin Films and powders of α-Fe ₂ O ₃	Sol-gel process followed by peptization of α-FeOOH peptized by glacial acetic acid	Iron nitrate Hydrate, 2-methoxy-ethanol and acetylacetone mixture, Ferric chloride/ammonia,	Differences in Local Crystalline order		13,14
8	Hollow spheres of Fe ₂ O ₃ powders	Spray pyrolysis & heat treatment under reduction-oxidation conditions	Aqueous Iron nitrate aerosols	Decomposition efficiency of nano- crystalline particles	--	15
9	Uniform sized γ- Fe ₂ O ₃ particles of different degree of crystallinity	Single step combustion process by spray pyrolysis	Fe-acetyl acetone, Fe-ammonium citrate, Fe-nitrate dissolved in methanol		Degree of crystallinity	16
10	Ferrite carbon composites	Pressure pyrolysis	Nickelocene and vinyl ferrocene	Thermo-magnetic properties	--	17
11	Nano-particles	Spray Pyrolysis			Spray Pyrolysis Mechanism	18

